Phosphomimetic substitution at Ser-33 of the chloroquine resistance transporter PfCRT reconstitutes drug responses in Plasmodium falciparum

Cecilia Sanchez, Sonia Moliner Cubel, Britta Nyboer, Monika Jankowska-Döllken, Christine Schaeffer-Reiss, Daniel Ayoub, Gabrielle Planelles, Michael Lanzer

JBC Papers in Press. Published on July 8, 2019 as Manuscript RA119.009464
The latest version is at http://www.jbc.org/cgi/doi/10.1074/jbc.RA119.009464

Phosphomimetic substitution at Ser-33 of the chloroquine resistance transporter PfCRT reconstitutes drug responses in *Plasmodium falciparum*

Cecilia P. Sanchez[1], Sonia Moliner Cubel[1], Britta Nyboer[1], Monika Jankowska-Döllken[1], Christine Schaeffer-Reiss[2], Daniel Ayoub[2,#], Gabrielle Planelles[3] and Michael Lanzer[1,*]

Running title: Phosphorylation of PfCRT affects drug transport kinetics

From the [1]Center of Infectious Diseases, Parasitology, Heidelberg University Hospital, Im Neuenheimer Feld 324, 69120 Heidelberg, Germany; the [2]Laboratoire de Spectrométrie de Masse BioOrganique, Université de Strasbourg, CNRS, IPHC UMR 7178, Strasbourg, France; and the [3]INSERM, Centre de Recherche des Cordeliers, Unité 1138, CNRS, ERL8228 Université Pierre et Marie Curie and Université Paris-Descartes, Paris, France

[#] Present address: Glenmark Pharmaceutical S.A., Chemin de la Combeta 5, 2300 La Chaux-de-Fonds, Switzerland

*To whom correspondence should be addressed: Michael Lanzer, Center of Infectious Diseases, Parasitology, Heidelberg University Hospital, Im Neuenheimer Feld 324, 69120 Heidelberg, Germany. Phone: ++49 6221 567845; Fax: ++49 6221 564643; E-mail: michael.lanzer@med.uni-heidelberg.de

Keywords: PfCRT, transport velocity, drug resistance, phosphorylation, genome editing, virulence factor, kinase inhibitor, posttranslational modification, malaria, Plasmodium

---

The chloroquine resistance transporter PfCRT of the human malaria parasite *Plasmodium falciparum* confers resistance to the former first line antimalarial drug chloroquine and it modulates the responsiveness to a wide range of quinoline and quinoline-like compounds. PfCRT is post-translationally modified by phosphorylation, palmitoylation, and, possibly, ubiquitination. However, the impact of these post-translational modifications on the *P. falciparum* biology and, in particular, on the drug resistance-conferring activity of PfCRT has remained elusive. Here, we confirm phosphorylation at Ser-33 and Ser-411 of PfCRT of the chloroquine resistant *P. falciparum* strain Dd2, and show that kinase inhibitors can sensitize drug responsiveness. Using CRISPR/Cas9 genome editing to generate genetically engineered PfCRT variants in the parasite, we further show that substituting Ser-33 with alanine reduced chloroquine and quinine resistance by approximately 50%, compared with the parental *P. falciparum* strain Dd2, whereas the phosphomimetic amino acid aspartic acid could fully, and glutamic acid partially, reconstitute the level of chloroquine/quinine resistance. Transport studies conducted in the parasite and in PfCRT-expressing *Xenopus laevis* oocytes linked phosphomimetic substitution at Ser-33 to increased transport velocity. Our data are consistent with phosphorylation of Ser-33 relieving an autoinhibitory intramolecular interaction within PfCRT, leading to a stimulated drug transport activity. Our findings shed additional light on the function of PfCRT and suggest that chloroquine could be reevaluated as an antimalarial drug by targeting the kinase in *P. falciparum* that phosphorylates Ser-33 of PfCRT.

The chloroquine resistance transporter PfCRT impinges on the susceptibility of the human malaria parasite *Plasmodium falciparum* to quinoline and quinoline-like antimalarial drugs, such as the former first line drug chloroquine and the currently deployed antimalarials quinine, amodiaquine, lumefantrine and piperaquine (1-8). In addition, PfCRT confers altered responses to a wide range of structurally unrelated compounds (9), including non-quinoline drug candidates in pre-clinical development (10). Given the importance of chemotherapy for malaria prevention and cure,

and taking into account that resistance to all classes of antimalarials is spreading, all efforts need to be made to prolong the longevity and efficacy of the existing arsenal of antimalarials and prevent the emergence of resistance to novel drugs. Such efforts would include a better understanding of the mechanism(s) by which PfCRT alters drug responses, not least because many of the drugs co-formulated with artemisinin as artemisinin combination therapy (the recommended treatment for uncomplicated malaria) are affected by PfCRT.

PfCRT belongs to the drug/metabolite transporter superfamily based on topology and sequence homology (11,12). Typical for this class, PfCRT features 10 predicted transmembrane domains and an internal pseudo symmetry, with both the C- and N-terminal domain facing the parasite's cytoplasm (13). PfCRT resides at the membrane of the parasite's digestive vacuole (8), a proteolytic organelle involved in the degradation of hemoglobin, which the parasite takes up from its host cell during intraerythrocytic development (14). PfCRT confers altered drug responses by acting as an efflux carrier expelling compounds from the digestive vacuole (15,16), where these compounds inhibit detoxification of the heme liberated as a result of hemoglobin digestion to inert hemozoin (14,17).

The mutational requirements converting PfCRT from a metabolite carrier, with a proposed specificity for iron, glutathione, basic amino acids or polyamines (18-20), into a drug transporting system have been extensively studied, revealing, e.g., the importance of the amino acid substitution of threonine for lysine at position 76 (3,21). The removal of the positively charged amino acid lysine in the transmembrane domain 1 of PfCRT is thought to provide access to, or generate, a multi-functional substrate binding pocket that can accommodate positively charged drugs, such as chloroquine and quinine, at distinct but interdependent binding sites (22). Other studies have described the role of additional mutations in augmenting the drug transport activity or balancing it with fitness costs (21,23,24). In total, PfCRT variants can carry between 4 to 10 amino acid substitutions, with geospecific signatures brought about by local histories of drug selection (5,25).

Less clear are the effects of posttranslational modifications on the activity of PfCRT. PfCRT is phosphorylated at several sites, including Ser-33, Ser-411, Thr-416 and Ser-420, as shown for the wild type form (13,26,27). It is palmitoylated at residue Cys-301 (28) and it is, possibly, ubiquitinated (6). The functional roles of these modifications are largely obscure. The only exception is the phosphorylation of Thr-416 that serves as a trafficking and sorting signal directing PfCRT from the ER to the digestive vacuolar membrane (13).

Given that phosphorylation is a powerful tool to regulate the activity of a carrier, as shown in other systems (29-32), we set out to interrogate the role of phosphorylation in the drug resistance-conferring activity of PfCRT. Our data show that phosphorylation of Ser-33 augments the level of PfCRT-conferred resistance to the antimalarial drugs chloroquine and quinine via a stimulation of the transport velocity.

Results

The kinase inhibitor ML-7 reverses chloroquine resistance

In an effort to complement studies conducted on wild type PfCRT (13,26,27), we initially examined the phosphorylation pattern of the drug resistance-conferring PfCRT variant ($PfCRT^{Dd2}$) from the chloroquine resistant *P. falciparum* strain Dd2. Nano-liquid chromatography coupled to tandem mass spectrometry identified phosphorylation of Ser-33, Ser-411 (Fig. 1A and B) and Thr-416 of $PfCRT^{Dd2}$. In addition to the phosphorylated forms, we also detected the unmodified amino acids. Phosphorylation of Ser-420 was not detected, only the unmodified form was observed.

To test the hypothesis of whether phosphorylation plays a role in the drug resistance-conferring activity of PfCRT, we screened 9 different kinase and one phosphatase inhibitor for an effect on chloroquine accumulation in Dd2. To this end, parasitized erythrocytes at the trophozoite stage (24-36 hrs post invasion) were incubated for 5 min in medium containing 42 nM [^{3}H]-chloroquine and the respective protein kinase or phosphatase inhibitor before the amount of label taken up was determined. The selected protein kinase inhibitors included inhibitors of protein kinases A and C (ML-7, ET-18-OCH3 and chelerythrine), casein kinases (TBB), calcium/calmodulin-dependent protein kinases (W7 and KN-93), tyrosine kinases (tryphostin A25) and general kinase inhibitors, such as H-89 and rottlerin (33,34), whereby the specificity and selectivity of these inhibitors are unclear in *P. falciparum*. As a phosphatase inhibitor, we used okadaic acid, a blocker of

serine/threonine protein phosphatases (35). As seen in Fig. 2A, only ML-7, W7, H-89 and rottlerin, significantly increased the amount of chloroquine taken up by the *P. falciparum* clone Dd2 ($p<0.05$, according to Student's t-test). Interestingly, three of the compounds, namely ML-7, W7, and H-89 are structurally related naphthalenesulfonamide and isoquinolinesulfonamide derivatives, whereas rottlerin is an unrelated natural polyphenolic compound.

We selected ML-7 for further analysis and tested the effect of increasing concentrations of ML-7, ranging from 0 to 30 µM, on chloroquine accumulation. The amount of chloroquine taken up by Dd2 increased with rising ML-7 concentrations until 10 µM before it declined, possibly, due to cytotoxic effects (Fig. 2B). In comparison, the chloroquine sensitive strain HB3 accumulated chloroquine to high levels in spite of ML-7 and only at toxic concentrations of >10 µM did the amount of chloroquine taken up decline (Fig. 2B). Comparable accumulation response profiles have been reported for verapamil and other chemosensitizers of chloroquine resistance (36).

We further evaluated the *in vitro* antiplasmodial activity of ML-7 in the standard growth inhibition assay and obtained IC_{50} values of 21 ± 4 µM and 36 ± 4 µM for Dd2 and HB3, respectively (Fig. 2C). An ML-7 concentration of 2.5 µM had only a mild, if any, cytotoxic effect on parasite development and was subsequently used in growth inhibition assays together with chloroquine or quinine. The addition of 2.5 µM ML-7 to the medium sensitized chloroquine resistance in Dd2, resulting in a significantly reduced chloroquine IC_{50} value - from 140 ± 10 nM, in the absence of ML-7, to 76 ± 4 nM in the presence of ML-7 ($p<0.001$, according to Student's t-test) (Fig. 3A). Similarly, ML-7 sensitized Dd2 to quinine, with quinine IC_{50} values dropping from 260 ± 15 nM to 130 ± 15 nM ($p<0.001$, according to Student's t-test) (Fig. 3B). In comparison, ML-7 did not affect the responsiveness of HB3 to chloroquine or quinine (Fig. 3A and B). As a control, we investigated the impact of ML-7 on pyrimethamine responsiveness. Pyrimethamine targets the dihydrofolate reductase/thymidylate synthase of the parasite and resistance to pyrimethamine is conferred by discrete point mutations in this bifunctional enzyme (37). No effects of ML-7 on pyrimethamine responses were found in HB3 and Dd2 (Fig. 3C). These data provide first evidence of phosphorylation possibly influencing PfCRT-mediated drug responses.

Phosphorylation of Ser-33 augments chloroquine and quinine resistance

To verify a role of phosphorylation in PfCRT-conferred drug responses, we attempted to substitute alanine for serine residues at position 33 and 411 in the sequence of PfCRT in Dd2, using trace-free genome editing technology via the CRISPR/Cas9 system (38). These two residues were chosen for further analysis because they were the predominant phosphorylation events with unknown function in the biology of PfCRT (see Fig. 1). In spite of numerous attempts we could not obtain the desired mutation for the S411A replacement. However, we were able to obtain the S33A mutation in several independent transfection experiments (Fig. 4A). Two independent clones, termed B5 S33A and B6 S33A, were subsequently isolated by limiting dilution and the desired mutation was confirmed by sequence analysis of the entire genomic *pfcrt* gene and the transcribed *pfcrt* mRNA (Fig. 4B). With the exception of the S33A substitution, PfCRT remained of the Dd2-type. Both mutants expressed PfCRT at the digestive vacuolar membrane, as shown by immuno-fluorescence assays using a specific rabbit antiserum to PfCRT (Fig. 5A). The total amount of PfCRT expressed in the two mutant clones was comparable to that of the parental Dd2 strain, according to semi quantitative Western analyses, with tubulin serving as an internal loading control (Fig. 5B).

Growth inhibition assays revealed a reduced level of chloroquine resistance in the B5 S33A and B6 S33A mutants to chloroquine as compared with Dd2, with IC_{50} values of 61 ± 3 nM, 60 ± 5 nM and 136 ± 5 nM, respectively ($p<0.001$, according to Holm-Sidak one way ANOVA test) (Fig. 6). The chloroquine sensitive *P. falciparum* clone HB3, which was analyzed in parallel assays, had an IC_{50} value of 14 ± 2 nM. Thus, the substitution of alanine for serine at position 33 within the PfCRT sequence of Dd2 resulted in an intermediate chloroquine resistance phenotype. Similarly, the two PfCRT S33A mutants were significantly more susceptible to quinine than was Dd2 and again displayed an intermediate response phenotype ($p<0.001$, according to Holm-Sidak one way ANOVA test) (Fig. 6). In contrast, the PfCRT S33A mutation did not affect the responsiveness to pyrimethamine (Fig. 6).

In order to mimic phosphorylation, we substituted Ser-33 by the negatively charged amino acids glutamic acid and aspartic acid, again using trace-free CRISPR/Cas9-mediated genome editing of the *pfcrt* gene in Dd2 (Fig. 4A). We obtained transfectants, and three clones each were selected for further analysis. These clones were termed F8 S33E, C8 S33E and B10 S33E, and A11 S33D, F8 S33D and G8 S33D, respectively. In each case, the nature of the amino acid substitution was confirmed by sequencing the *pfcrt* gene and the corresponding transcript (Fig. 4B). All mutants expressed PfCRT at the digestive vacuolar membrane at overall expression levels comparable to that of the parental clone Dd2 (Fig. 5A and B).

Interestingly, the S33E and the S33D mutants displayed different response phenotypes with regard to chloroquine and quinine. All S33E mutants had chloroquine and quinine IC_{50} values that were slightly, but significantly, higher than those of the S33A mutants, but did not reach the level of resistance displayed by Dd2 ($p<0.001$, according to Holm-Sidak one way ANOVA test) (Fig. 6). In contrast, all S33D mutants revealed chloroquine and quinine IC_{50} values that were statistically indistinguishable from that of Dd2 ($p>0.1$ according to Holm-Sidak one way ANOVA test) (Fig. 6). These findings suggest that aspartic acid can substitute fully, and glutamic acid partially, for Ser-33, respectively phosphoserine, within PfCRT. Verapamil, a partial mixed type inhibitor of PfCRT (22), could sensitize chloroquine responsiveness in all mutants (Fig. 6). The responses of the mutants to pyrimethamine were unaffected by the mutational changes introduced in the PfCRT sequence (Fig. 6).

Phosphorylation stimulates the transport velocity of PfCRT

To better define the mechanism by which phosphorylation affects PfCRT-conferred drug responses, we expressed the PfCRT variants in *Xenopus laevis* oocytes. In all cases, PfCRT co-localized with the established oolemma marker inositol 1,4,5-triphosphate receptor (InsP3R), as shown by immuno-fluorescence assays (Fig. 7A), and semi-quantitative Western analyses revealed comparable expression levels relative to the internal standard α-tubulin (Fig. 7B). Water-injected oocytes did not react with the PfCRT-specific antiserum.

All PfCRT expressing oocytes displayed saturable chloroquine uptake kinetics when incubated in an acidic buffer of pH 6.0 containing increasing concentrations of radiolabeled chloroquine ranging from 0 to 500 µM (Fig. 7C). However, there were clear distinctions with regard to the specific kinetic parameters, as revealed by fitting the Michaelis Menten equation to the data points (Fig. 7C). For $PfCRT^{Dd2}$ a K_m of 250 ± 40 µM and a V_{max} of 33 ± 3 pmol oocyte^{-1} h^{-1} were obtained, consistent with previous reports (15,22,39) (Table 1). Interestingly, the Ser-33 mutants had K_m values comparable to that of $PfCRT^{Dd2}$ but significantly different V_{max} values, with the S33A mutant displaying the lowest V_{max} of 22 ± 2 pmol oocyte^{-1} h^{-1}, the S33E mutant an intermediate value of 26 ± 1 pmol oocyte^{-1} h^{-1} and the S33D mutant a V_{max} comparable to that of $PfCRT^{Dd2}$ ($p<0.01$, according to Holm-Sidak one way ANOVA test and F-statistics) (Table 1). These findings suggest that phosphorylation of Ser-33 stimulates PfCRT-mediated drug efflux via an increase in transport velocity.

To support this hypothesis, we performed chloroquine efflux experiments in the parasite (16). To this end, parasitized erythrocytes at the trophozoite stage were incubated with 100 nM [^{3}H]-chloroquine for 15 min, washed and then incubated in fresh medium before aliquots were taken at defined time points to determine the chloroquine efflux kinetics. As seen in Fig. 7D, preloaded chloroquine is rapidly released from erythrocytes infected with Dd2 with an initial rate of 0.71 ± 0.03 min^{-1} (Table 2), consistent with previous reports (16). In comparison, chloroquine efflux was slow in the presence of verapamil or in erythrocytes infected with the chloroquine sensitive *P. falciparum* strain HB3 (16) (Fig. 7D). Interestingly, the Ser-33 mutants displayed different drug efflux phenotypes (Fig. 7D). Whereas the efflux kinetics of the PfCRT S33D mutant was comparable to that of Dd2, the S33A mutant expelled chloroquine with a significantly lower rate of 0.43 ± 0.04 min^{-1} ($p<0.01$ according to an F-test) (Table 2 and Fig. 7D). The PfCRT S33E mutant displayed a trend towards a slightly reduced chloroquine efflux phenotype.

Discussion

PfCRT is a multisite phosphoprotein, with both the N- and C-terminal cytoplasmic domain being post-translationally modified by the addition of a phosphate group (13,26,27), as confirmed in this study for the PfCRT variant of the chloroquine resistant strain Dd2 (Fig. 1). A phosphate group can change the conformation of

a protein due to its negative charge, which, in turn, can activate or inhibit the protein or affect its interaction with other factors, as shown in other systems including carriers (29-31). In the case of PfCRT, evidence is amounting that phosphorylation likewise plays a crucial role in the biology of this transporter and that discrete phosphorylation events exert defined and distinct functionalities. For instance, phosphorylation of Thr-416 is a necessary, deciding signal for the trafficking of the transporter from the ER to its final destination, the digestive vacuolar membrane (13). In the absence of this signal, PfCRT is mistargeted to the parasite's plasma membrane (13). In the present study, we present evidence suggesting a modulatory effect of Ser-33 phosphorylation on the drug resistance-conferring activity of PfCRT.

The conclusion of phosphorylation augmenting PfCRT-conferred drug responses is supported by pharmacological, genetic and biochemical evidence. Firstly, the established protein kinase inhibitors ML-7, W7, H-89 and rottlerin were found to sensitize chloroquine and quinine responsiveness in the *P. falciparum* strain Dd2, resulting in increased drug accumulation levels (as shown for all four protein kinase inhibitors) (Fig. 2A) and decreased IC_{50} values (as exemplified by ML-7) (Fig. 3A and B), although such effects might also result from these kinase inhibitors impairing trafficking of PfCRT to the digestive vacuole. Secondly and more importantly, genetically engineered phosphomimetic substitution mutants provided a direct and causative link between phosphorylation of Ser-33, and the responsiveness of the parasite to the two PfCRT substrates chloroquine and quinine. PfCRT mutants in which Ser-33 was substituted by alanine, displayed an approximately 50% reduction in the chloroquine and quinine IC_{50} values, as compared with the parental strain Dd2 (Fig. 6). Alanine lacks a hydroxyl group on its carbon side chain but otherwise has an overall structural similarity to serine. In comparison, PfCRT mutants carrying the phosphoserine mimicking amino acid aspartic acid displayed IC_{50} values comparable to that of Dd2 (Fig. 6). The finding that aspartic acid, unlike glutamic acid, could fully replace Ser-33 can be explained by the closer structural similarity between phosphoserine and aspartic acid than between phosphoserine and glutamic acid.

All PfCRT mutants were generated using CRISPR/Cas9 mediated genome editing technology in such a manner that specifically introduced the desired mutation, but otherwise left no trace. Thus, the *pfcrt* gene itself and the surrounding chromosomal locus remained intact. The trace-free transfection strategy distinguishes our approach from previous attempts to genetically manipulate the *pfcrt* gene, which altered the intron/exon structure of the gene, inserted selection cassettes into the chromosomal domain or resulted in duplication and/or deletion events (3,40), with unpredictable consequences for gene expression and protein synthesis. Since our approach leaves the chromosomal organization intact, the observed drug responses can be directly ascribed to the specific PfCRT mutations. Regardless, we determined the steady-state PfCRT protein level as well as the subcellular location of the transporter at the digestive vacuolar membrane, and found no differences between the mutants and the parental Dd2 strain (Fig. 5). Similarly, no differences in expression levels were observed for the PfCRT variants expressed in the *X. laevis* oocyte system (Fig. 7B). We further did not note differences in protein trafficking. These findings are consistent with previous reports showing that the N-terminal cytoplasmic domain of PfCRT does not contribute to the sorting and trafficking of the transporter to the digestive vacuole in the parasite (13).

Thus, the differential levels of drug resistance cannot be explained by altered expression or aberrant trafficking of PfCRT from intracellular pools to the digestive vacuolar membrane. Instead, our data suggest that the phenotypic alterations are a consequence of the effect phosphorylation of Ser-33 has on the activity of PfCRT. This conclusion is further corroborated by biochemical evidences, showing that the PfCRT-conferred drug efflux rate is significantly reduced in the parasite when Ser-33 is replaced by alanine, but fully reconstituted by the phosphomimetic amino acid aspartic acid (Fig. 7D and Table 2). Moreover, kinetic studies conducted in the *Xenopus* oocyte system mechanistically link the effect of Ser-33 on drug responses to a stimulation of the PfCRT-mediated drug transport velocity, with the S33A mutant displaying a significantly reduced V_{max} value compared to $PfCRT^{Dd2}$ while maintaining a comparable K_m value (Fig. 7C and Table 1). Again, the impaired drug transport velocity can be fully reconstituted by aspartic acid and partially by glutamic acid (Fig. 7C and Table 1).

On the basis of our findings we hypothesize that Ser-33 phosphorylation relieves an autoinhibitory intramolecular interaction, thereby stimulating the drug transporting activity of PfCRT. The proposed spatial proximity of the N-terminal cytoplasmic domain of PfCRT with the putative drug binding pocket contained in the transmembrane domain 1 might facilitate autoinhibitory interactions (41). As attractive as such a model might be, it awaits verification by crystallographic data on the three-dimensional structure of PfCRT.

Whether a similar autoinhibitory mechanism operates in the non-drug transporting, wild type PfCRT form remains to be seen and would require in-depth knowledge regarding the natural substrate. However, a consensus has yet to be reached as to the nature of the non-drug related substrate, with possible candidates ranging from ferrous and ferric iron to glutathione and positively charged amino acids (18-20). Further, it is by no means certain that Ser-33 increases the transport activity of PfCRT for its natural substrate since phosphorylation can have diverging, solute specific effects on transporters, as shown in other systems (42).

While our findings causatively link phosphorylation of Ser-33 with the drug resistance function of PfCRT, they do not disclose the identity of the kinase involved in this process. The kinase inhibitors used in this study are ill characterized in *P. falciparum* and studies conducted in other systems have demonstrated that kinase inhibitors often lack selectivity and specificity (33,34). For instance, ML-7 is classified as a selective mammalian myosin light chain kinase inhibitor (MLCK) (34,43), but it also inhibits human CK2α, PKA and PKC, albeit at higher concentrations (44). In the *P. falciparum* system, ML-7 was shown to inhibit recombinant CK2, but so does TBB (44), which, unlike ML-7 and rottlerin, had no statistically significant effect on chloroquine accumulation (Fig. 2A). H-89 targets mammalian PKA and also many other kinases, including S6K1, MSK1, ROCK-II, PKBα, MAPKAP-K1b and MLCK (33,45). W7 is a calmodulin antagonist that inhibits MLCK (46,47). One may extract MLCK as a common denominator from the inhibition profiles. However, *P. falciparum* lacks orthologues of MLCKs. The closest relatives are members of the calcium-dependent protein kinase (CDPK) family (48).

There are computational programs that predict phosphorylation sites and the corresponding protein kinase based on sequence information. However, such analysis tools have been trained on mammalian or yeast phosphorylation sites and kinases and their predictive value for *P. falciparum* has yet to be established. In the case of PfCRT, several of the bioinformatics tools, including NetPhos 3.1 and GPS 3.0, recognized Ser-33 as a phosphorylation site but failed to assign a specific kinase with sufficient statistical confidence. Thus, the nature of the kinase that acts on Ser-33 is elusive and, although CDPKs are possible candidates, none of the protein kinases encoded in the *P. falciparum* genome should be excluded at present (48). Our study encourages efforts to identify this kinase, not least because the kinase is an attractive drug target. Inhibiting this kinase might sensitize the resistant parasites to chloroquine and quinine, thus providing new opportunities for revitalizing or prolonging the longevity and efficacy of these drugs. In summary, our studies reveal a novel aspect in the biology of PfCRT, by suggesting that a specific phosphorylation event regulates the drug-resistance conferring activity of PfCRT via a stimulation of the transport velocity.

Experimental Procedures

Ethics approval

The study procedure used in the experimentation for this manuscript in surgical removal of stage V-VI oocytes from *Xenopus laevis* frogs was approved by the Regierungspräsidium Karlsruhe (Aktenzeichen 35-9185 81/G-31/11 and 35-9185.81/G-276/15) in accordance with the German "Tierschutzgesetz.".

Chemicals

[^{3}H]chloroquine (specific activity 25 Ci mmol^{-1}) was purchased from American Radiolabeled Chemicals. Protein kinase and phosphatase inhibitors were obtained from Sigma-Aldrich.

P. falciparum culture

P. falciparum strains were cultured as described (49), using RPMI medium supplemented with 5% human serum, 0.25% Albumax II (Gibco, Germany), 200 µM hypoxanthine and 20 µg/ml gentamycin. Cultures were synchronized by D-sorbitol lysis (50). Cultures were free of mycoplasma as determined using the Venor GeM Classic kit (Minerva Biolabs).

Mass spectrometry

Mass spectrometry of PfCRT was performed as previously described in detail (13). Briefly, infected erythrocytes of the *P. falciparum* strain Dd2 at the trophozoite stage expressing episomally a $PfCRT^{Dd2}$/GFP fusion protein were purified from 600 ml parasite culture (5% hematocrit and 8% parasitemia) using the Super MACS magnet (Miltenyi Biotech) and the D column. Infected erythrocytes were subsequently treated with 0.1% saponin in PBS. Total proteins were extracted from the parasite pellet, using RIPA buffer (1% NP-40, 1% sodium deoxycholate, 0.1% SDS, 150 mM NaCl, 10 mM Na-phosphate buffer pH 7, 1 mM EDTA). The lysate was then diluted with 9 volumes of NETT buffer (10 mM Na-phosphate buffer pH 7, 150 mM NaCl, 0.1% NP-40, and 1 mM EDTA) and the $PfCRT^{Dd2}$/GFP fusion protein was immuno-precipitated using a goat anti-GFP antiserum. Immuno-precipitated material was washed in buffers with increasing NaCl concentrations ranging from 250 to 350 mM and one additional wash with 10 mM Na-phosphate buffer pH 7 before being size-fractionated by SDS-PAGE (10% acrylamide, 6M Urea). The gel was stained in Imperial Protein stain (Pearce) and slices of 2 mm width were excised around the projected molecular weight of PfCRT. All buffers used were supplemented with a cocktail of protease and phosphatase inhibitors (50 µg ml^{-1} aprotinin, 20 µg ml^{-1} leupeptin, 1 mM PMSF, 50 mM NaF, 0.2 mM $NaVO_3$). The gel slices were prepared using a MassPREP automated system (Waters). The gel slices were washed twice in 25 mM ammonium hydrogen carbonate and acetonitrile. The cysteine residues were subsequently reduced in 10 mM dithiothreitol at 57°C and then alkylated in 55 mM iodoacetamide. After dehydration with acetonitrile, the proteins were cleaved in gel using 12.5 ng/µl of modified porcine trypsin (Promega) in 25 mM NH_4HCO_3 at 37°C overnight. The tryptic peptides were extracted twice, using 0.4% CF_3CO_2H in CH_3CN/H_2O (60/40) for the first extraction and 100% CH_3CN for the second extraction. The volumes were then reduced to 5 µl by speed vacuuming to eliminate acetonitrile and to concentrate the peptides. Samples were analyzed using an Agilent 1200 series HPLC-Chip/MS system (Agilent Technologies) coupled to an HCT Plus ion trap mass spectrometer (Bruker Daltonics), as previously described (13). MS/MS data sets were processed using the Mascot search engine (Matrix Science) (13). Spectra were searched with a mass tolerance of 0.5 Da for MS and MS/MS data, allowing for a maximum of one missed cleavage with trypsin and with carbamidomethylation of cysteines, oxidation of methionines, acetylation of protein N-terminal, phosphorylation of serines, threonines and tyrosines specified as variable modifications. Searches were performed against an in house generated composite target-decoy database containing NCBI protein sequences of *P. falciparum*. The spectra of the phosphorylated peptides of PfCRT were manually re-inspected.

Primers

The sequences of the primers used for site directed mutagenesis of *pfcrt* are compiled in the supplementary Table S1.

Site-directed mutagenesis of *pfcrt* in *P. falciparum*

To introduce the desired mutational changes in the *pfcrt* sequence, we used the previously described CRISPR/Cas9 genome editing technology (38). The desired mutational changes were introduced, using the overlap extension method (51) and the appropriate primer pairs. To this end, the region of the *pfcrt* gene from -120 to +780 was amplified from genomic DNA of Dd2 using the following primer pairs: for the S33A mutation, N° 1/4 and N° 3/2; for the S33E mutation N° 1/6 and N° 5/2; and for the S33D mutation N° 1/8 and N° 7/2. The two PCR products were then used as a template for amplification of the final product using the primer pair N° 1 and N° 2. The fragment was subsequently cloned into pJET and further into the transfection vector pL6-CS (38). The desired mutation was confirmed by sequencing. The double stranded oligonucleotide encoding the PfCRT-specific guide RNA (N° 9 and N° 10) was cloned into the appropriate region of the transfection vector pL6-CS via In-Fusion Cloning (Clontech).

Transfection

P. falciparum ring stages were transfected by electroporation with 75 µg each of the pL6 and pUF1-Cas9 transfection vector, as described previously (52). Transfectants appeared after 5 – 8 weeks of selection using 5 nM WR99210 and 1.5 µM DSM1. Clonal lines were selected by limiting dilution. The sequence of the *pcrt* gene was confirmed for each selected clone by sequencing, using primer N° 11, following amplification from genomic DNA using the

primers N° 1 and N° 12. In addition, the corresponding *pfcrt* transcript was confirmed by sequencing following reverse transcription of the mRNA.

Chloroquine accumulation assay

Chloroquine accumulation by *P. falciparum* infected erythrocytes (trophozoites) was performed as described (53). Briefly, magnet-purified trophozoite-infected erythrocytes were resuspended in transport buffer (bicarbonate-free RPMI 1640 containing 11 mM glucose and supplemented with 25 mM HEPES-Na and 2 mM glutamine, pH 7.3 at 37 °C) containing 42 nM [^{3}H]-chloroquine and the indicated protein kinase or phosphatase inhibitor (at concentrations indicated in Fig. 2A) at a hematocrit of 30 000 cells μl^{-1}. The hematocrit was determined using a Coulter Counter (Z1-Coulter Particle Counter, Beckman Coulter Inc.). The cells were then incubated at 37 °C for 5 min before duplicative 75 µL aliquots were removed from the reaction and spun through a layer of a 5:4 mixture of dibutyl phthalate and dioctyl phthalate (15000g, 5 s) to separate the cells from the aqueous medium, which contained the unincorporated [^{3}H]-chloroquine. The radioactivity contained in the supernatant and in the cell pellet was subsequently determined using a liquid scintillation counter (TRI-CARB 2100 TR, Packard). Chloroquine accumulation was then expressed as the ratio of the intracellular versus the extracellular chloroquine.

Chloroquine efflux assay

Chloroquine efflux kinetics were determined as described (16). Briefly, magnet purified *P. falciparum*-infected erythrocytes at the trophozoite stage were resuspended in transport buffer (see above) at a hematocrit of approximately 25,000 cells μl^{-1}. [^{3}H]-chloroquine was added to a final concentration of 100 nM and the cells were incubated at 37°C for 15 minutes. Cells were then washed twice in ice-cold transport buffer (pH adjusted to 7.3 at 4°C) before they were resuspended in prewarmed transport buffer at a hematocrit of 9,000 cells μl^{-1}. 150 µl aliquots were withdrawn at the time points indicated and the amount of extracellular and intracellular [^{3}H]-chloroquine was determined as described above. The initial efflux rate was determined by plotting the amount of intracellular chloroquine as a function of time and fitting a single, three parameter exponential decay equation to the data points.

IC_{50} determination

Cell proliferation assays in the presence of different concentrations of chloroquine, quinine, and pyrimethamine, were performed according to the standard SYBR green fluorescence-based assay (54). At the day of the experiment, the culture was adjusted to a parasitemia of 0.5 % (rings) and a hematocrit of 3%. Parasite growth was assessed after 72 hr exposure time. Cells were lysed in lysis buffer (20 mM Tris-HCl, 5 mM EDTA, 0.008% saponin, 0.08% triton X-100, pH 7.4) containing SYBR green. Fluorescence was determined using a FLUOstar OPTIMA plate reader with the following settings: excitation wavelength: 485 nm; emission wavelength: 520 nm; gain: 1380; nº of flashes/well: 10; top optic. Growth inhibition assays were performed by three different researchers over a period of 18 months.

Western blot

Magnet purified trophozoites were saponin-lysed (0.07% in PBS, 1 mM PMSF, 50 µg/ml aprotinin, 20 µg/ml leupeptin), washed two times in PBS and solubilized using protein loading buffer (250 mM Tris pH 6.8, 3% SDS, 20% glycerol, 0.1% Bromophenol blue). Supernatant fractions were collected after centrifugation (17,000 g for 30 min at 4°C) and subsequently analyzed by SDS-PAGE. Gels were transferred to an Immun-Blot® PVDF membrane (Bio-Rad) using an iBlot2 transfer apparatus. The following antibodies were used: mouse anti-α-tubulin (1:1000 dilution; clone B-5-1-2; Sigma Aldrich), rabbit anti-PfCRT (1:1000 dilution) (8), donkey anti-mouse-POD (1:10000 dilution; Abcam) and goat anti-rabbit-POD (1:10000 dilution; Abcam). All antibodies were diluted in 1% (w/v) BSA in PBS. The signal was captured with a blot scanner (C-DiGit from Li-Cor).

Immuno-fluorescence assay

Magnetic purified trophozoites were washed once with PBS and fixed with 4% paraformaldehyde and 0.0075% glutaraldehyde in PBS for 30 min. The samples were centrifuged (all the centrifugations were carried out at 600 x g for 2 min) and the pellets were resuspended in, and incubated with, 0.1% (v/v) Triton in PBS for 15 min. After a washing step with PBS, the samples were neutralized during 10 min with 10 mM NH_4Cl pH 7.0. The infected erythrocytes were washed once with PBS and once with 3% (w/v) BSA in PBS. A 3% (w/v) BSA in PBS solution was used for the blocking and washing

steps, and to dilute the antibodies. The samples were blocked for 2 hrs. The incubation with rabbit anti-PfCRT antibody (1:1000 dilution) was carried out for 90 min. Infected erythrocytes were washed 3 times and incubated with donkey anti-rabbit Alexa Fluor 488 secondary antibody (1:1000 dilution; Thermo Scientific) for 45 min. The samples were then washed again 3 times and kept over-night in PBS at 4ºC until they were imaged in a perfusion chamber using an LSM 510 confocal microscope (Zeiss). The samples were excited using a 488 nm Argon ion laser and the emission was detected using a 505-550 nm band pass filter. The objective used was a C-Apochromat with 63 x magnification. The images were acquired using the LSM imaging software and processed with the FIJI program.

PfCRT expression in *Xenopus laevis* oocytes

Oocytes were obtained as previously described (18). Briefly, adult female *X. laevis* frogs (purchased from NASCO) were anaesthetized by submersion in a cooled solution of ethyl 3-amino benzoate methanesulfonate (0.3%, w/v) before parts of the ovary were surgically removed. The ovaries were carefully pulled apart into small pieces, which were gently shaken for 14-16 hours at 18°C in Ca^{2+}-free ND96 buffer supplemented with Collagenase D (0.1 % w/v, Roche), BSA (0.5% w/v) and 9 mM Na_2HPO_4. After collagenase treatment oocytes were washed with ND96 buffer (96 mM NaCl, 2 mM KCl, 1.8 mM $CaCl_2$, 1 mM $MgCl_2$, buffered with 5 mM HEPES, pH 7.5 and supplemented with 100 mg l^{-1} gentamycin) and defolliculated, healthy-looking stage V-VI oocytes were selected for microinjection. RNA for injection was generated using the codon-optimized coding sequence of $PfCRT^{Dd2}$ subcloned into the pSP64T expression vector, which was subsequently linearized using the restriction endonucleases BamHI or SalI (New England Biolabs GmbH, Frankfurt, Germany) and transcribed *in vitro* using the mMESSAGE mMACHINE™ SP6 Transcription Kit (Thermo Fisher Scientific). The RNA was stored at -80°C and diluted with nuclease-free water to the desired concentration of 0.6 µg $µl^{-1}$. RNA was injected using precision-bore glass capillary tubes (3.5'' glass capillaries, Drummond Scientific Company), which were pulled on a vertical puller (P-87 Flaming/Brown micropipette puller, Sutter instrument). The micropipettes were connected to a microinjector (Nanoject II Auto-Nanoliter Injector, Drummond Scientific company). Injection was conducted under stereo microscopic control. 50 nl nuclease-free water alone (control oocytes) or 50 nl nuclease-free water containing 30 ng RNA were injected per oocyte. Injected oocytes were kept for 48-72 hours at 18°C in ND96 buffer with daily buffer changes before being used for further experiments.

Site-directed mutagenesis of *pfcrt* for expression in *X. laevis* oocytes

A codon-optimized coding sequence of $PfCRT^{Dd2}$ was subcloned into the SP64T expression vector (15). To introduce the desired mutational changes into the *pfcrt* sequence, the overlap extension method was used. A region from the 5`untranslated *Xenopus* beta-globin sequence to the respective 3´region flanking the *pfcrt* sequence was amplified using the following primer pairs: for the S33A mutation, N° 13/16 and N° 14/15, for the S33E mutation, N° 13/18 and N° 14/17, for the S33D mutation, N° 13/20 and N° 14/19 (primers, see supplementary Table S1). Both PCR products were used as template for amplification of the final product using the primer pair N° 13/14. The resulting fragment was cloned into the SP64T expression vector and the desired mutation was confirmed by sequencing.

Chloroquine uptake kinetics

Chloroquine flux assays were performed as previously described (15,18,22,39). Briefly, oocytes were incubated for 60 min at room temperature in ND96 buffer (buffered with 5 mM MES/Tris base for pH 6), containing 42 nM [^{3}H]-chloroquine and 10-500 nM of unlabeled chloroquine. To determine the amount of chloroquine taken up by each oocyte, the radioactive medium was removed and oocytes were washed three times in ice-cold ND96 buffer. Each oocyte was transferred into a scintillation vial and was lysed by adding 200 µl of a 5% SDS solution. The radioactivity of each sample was measured using a LS 6000 IC Liquid Scintillation Counter (Beckman Coulter). The direction of transport in this assay is from the extracellular medium (pH 6) into the oocyte cytosol (pH 7.2), which corresponds to the efflux of chloroquine from the acidic digestive vacuole (pH 5.2) into the parasite cytosol (pH 7.2). Water-injected oocytes were analyzed in parallel. The specific PfCRT-mediated uptake was determined by subtracting the background uptake from water-injected oocytes from that of PfCRT-expressing oocytes. In all cases, at least three separate experiments were performed, i.e. on oocytes from

different frogs, and in each experiment, measurements were made from 10 oocytes per treatment.

Western Blot analysis of oocyte lysates

Oocyte lysates were generated as described (55). Briefly, 3 days after RNA injection, total lysates were prepared from *X. laevis* oocytes by the addition of 20 µl homogenization buffer (20 mM HEPES) per oocyte supplemented with protease inhibitor cocktail (Roche). Cellular debris was removed by centrifugation at 800g for 5 minutes at room temperature. Supernatants were stored at -80°C and mixed with 2x sample buffer (250 mM Tris pH 6.8, 3% SDS, 20% glycerol, 0.1% Bromophenol blue) before the extracts were size-fractionated using 12% SDS-PAGE and transferred to a polyvinylidene difluoride membrane. The following antibodies were used: monoclonal mouse anti-α-tubulin (1:1000 dilution; clone B-5-1-2; Sigma-Aldrich), guinea pig anti-PfCRT antiserum (raised against the N terminus of PfCRT (MKF ASK KNN QKN SSK), 1:1000 dilution, Eurogentec), goat anti-mouse-POD (1:10000 dilution; Jackson Immuno Research) and donkey anti-guinea pig-POD (1:10000 dilution; Jackson Immuno Research). All antibodies were diluted in 1% (w/v) BSA in PBS. The signal was captured with a blot scanner (C-DiGit from Li-Cor).

Immuno-fluorescence assay of oocytes

Three days after RNA injection, oocytes were fixed with 4% (v/v) paraformaldehyde in PBS for 4 hrs at room temperature. Fixed cells were washed three times with 3% (w/v) BSA in PBS and subsequently permeabilized with 0.05% (v/v) Triton-X 100 in PBS for 60 min. Oocytes were washed three times with 3% (w/v) BSA in PBS and incubated with a rabbit polyclonal antiserum raised against InsP3R-I (H-80, 1:200 dilution, Santa Cruz) and the guinea pig anti-PfCRT antiserum (1:500 dilution) overnight at 4°C. Oocytes were washed again, before the anti-rabbit Alexa Fluor 546 secondary antibody (1:1000 dilution, Invitrogen) and the anti-guinea pig Alexa Fluor 488 secondary antibody (1:1000 dilution, Invitrogen) were added for 90 min at room temperature. All antibodies were diluted in 3% (w/v) BSA in PBS. Cells were washed three times before they were analyzed by fluorescence microscopy. Images were taken with a Zeiss LSM 510 confocal microscope (Zeiss). The images were acquired using the LSM imaging software and processed with the FIJI program.

Statistics and reproducibility

Statistical analyses were performed, using the Sigma Plot (v.13, Systat) software. Statistical significance was determined using the Holm-Sidak one way ANOVA test, the Student's t-test or the F-test, where appropriate. The number of independent biological replicates is indicated in the main text and/or the figure legends, and in most cases corresponds to the number of individual date points depicted in the graph. If independent data points are averaged, then the mean ± standard error is shown. Independent biological replicates are defined as independent infections using blood from different donors or independent experiments using oocytes from a different frog.

Data availability

The original data underlying this article are compiled in the supplementary Table 2.

Acknowledgement

The research leading to these results have received funding from the joint French-German Research Initiative sponsored by the Agence Nationale de la Recherche (ANR) and the Deutsche Forschungsgemeinschaft (DFG) (EVOTRANSPORT / ANR-14-CE35-0012-01 and LA 941/11-1) and the PHC PROCOPE (30995WE and ID 57051467). G.P. acknowledges the generous support by the INSERM, CNRS, and the Université Paris-Descartes. C.S.R thanks the Proteomic French Infrastructure (ProFI ; ANR-10-INSB-08-03) for financial support. M.L. is a member of the research cluster of excellence CellNetworks. S.M.C. was a PhD student at the HBIGS graduate school at Heidelberg University. We thank Justine Schneider for re-processing the MS/MS data and Marina Müller for excellent technical assistance.

Competing financial interests

The authors declare that they have no conflicts of interest with the contents of this study.

References

1. Agrawal, S., Moser, K. A., Morton, L., Cummings, M. P., Parihar, A., Dwivedi, A., Shetty, A. C., Drabek, E. F., Jacob, C. G., Henrich, P. P., Parobek, C. M., Jongsakul, K., Huy, R., Spring, M. D., Lanteri, C. A., Chaorattanakawee, S., Lon, C., Fukuda, M. M., Saunders, D. L., Fidock, D. A., Lin, J. T., Juliano, J. J., Plowe, C. V., Silva, J. C., and Takala-Harrison, S. (2017) Association of a novel mutation in the *Plasmodium falciparum* chloroquine resistance transporter with decreased piperaquine sensitivity. *J Infect Dis* **216**, 468-476
2. Dhingra, S. K., Redhi, D., Combrinck, J. M., Yeo, T., Okombo, J., Henrich, P. P., Cowell, A. N., Gupta, P., Stegman, M. L., Hoke, J. M., Cooper, R. A., Winzeler, E., Mok, S., Egan, T. J., and Fidock, D. A. (2017) A variant *pfcrt* isoform can contribute to *Plasmodium falciparum* resistance to the first-line partner drug piperaquine. *MBio* **8**, 10.1128/mBio.00303-17
3. Lakshmanan, V., Bray, P. G., Verdier-Pinard, D., Johnson, D. J., Horrocks, P., Muhle, R. A., Alakpa, G. E., Hughes, R. H., Ward, S. A., Krogstad, D. J., Sidhu, A. B., and Fidock, D. A. (2005) A critical role for pfcrt k76t in *Plasmodium falciparum* verapamil-reversible chloroquine resistance. *EMBO J* **24**, 2294-2305
4. Johnson, D. J., Fidock, D. A., Mungthin, M., Lakshmanan, V., Sidhu, A. B., Bray, P. G., and Ward, S. A. (2004) Evidence for a central role for *pfcrt* in conferring *Plasmodium falciparum* resistance to diverse antimalarial agents. *Mol Cell* **15**, 867-877
5. Sa, J. M., Twu, O., Hayton, K., Reyes, S., Fay, M. P., Ringwald, P., and Wellems, T. E. (2009) Geographic patterns of *Plasmodium falciparum* drug resistance distinguished by differential responses to amodiaquine and chloroquine. *Proc Natl Acad Sci U S A* **106**, 18883-18889
6. Sanchez, C. P., Liu, C. H., Mayer, S., Nurhasanah, A., Cyrklaff, M., Mu, J., Ferdig, M. T., Stein, W. D., and Lanzer, M. (2014) A HECT ubiquitin-protein ligase as a novel candidate gene for altered quinine and quinidine responses in *Plasmodium falciparum*. *PLoS Genet* **10**, e1004382
7. Sanchez, C. P., Mayer, S., Nurhasanah, A., Stein, W. D., and Lanzer, M. (2011) Genetic linkage analyses redefine the roles of *pfcrt* and *pfmdr1* in drug accumulation and susceptibility in *Plasmodium falciparum*. *Mol Microbiol* **82**, 865-878
8. Fidock, D. A., Nomura, T., Talley, A. K., Cooper, R. A., Dzekunov, S. M., Ferdig, M. T., Ursos, L. M., Sidhu, A. B., Naude, B., Deitsch, K. W., Su, X. Z., Wootton, J. C., Roepe, P. D., and Wellems, T. E. (2000) Mutations in the *P. falciparum* digestive vacuole transmembrane protein PfCRT and evidence for their role in chloroquine resistance. *Mol Cell* **6**, 861-871
9. Yuan, J., Cheng, K. C., Johnson, R. L., Huang, R., Pattaradilokrat, S., Liu, A., Guha, R., Fidock, D. A., Inglese, J., Wellems, T. E., Austin, C. P., and Su, X. Z. (2011) Chemical genomic profiling for antimalarial therapies, response signatures, and molecular targets. *Science* **333**, 724-729
10. van Schalkwyk, D. A., Nash, M. N., Shafik, S. H., Summers, R. L., Lehane, A. M., Smith, P. J., and Martin, R. E. (2016) Verapamil-sensitive transport of quinacrine and methylene blue via the *Plasmodium falciparum* chloroquine resistance transporter reduces the parasite's susceptibility to these tricyclic drugs. *J Infect Dis* **213**, 800-810
11. Martin, R. E., and Kirk, K. (2004) The malaria parasite's chloroquine resistance transporter is a member of the drug/metabolite transporter superfamily. *Mol Biol Evol* **21**, 1938-1949
12. Tran, C. V., and Saier, M. H., Jr. (2004) The principal chloroquine resistance protein of *Plasmodium falciparum* is a member of the drug/metabolite transporter superfamily. *Microbiology* **150**, 1-3
13. Kuhn, Y., Sanchez, C. P., Ayoub, D., Saridaki, T., van Dorsselaer, A., and Lanzer, M. (2010) Trafficking of the phosphoprotein PfCRT to the digestive vacuolar membrane in *Plasmodium falciparum*. *Traffic* **11**, 236-249
14. Coronado, L. M., Nadovich, C. T., and Spadafora, C. (2014) Malarial hemozoin: From target to tool. *Biochim Biophys Acta* **1840**, 2032-2041
15. Martin, R. E., Marchetti, R. V., Cowan, A. I., Howitt, S. M., Broer, S., and Kirk, K. (2009) Chloroquine transport via the malaria parasite's chloroquine resistance transporter. *Science* **325**, 1680-1682

16. Sanchez, C. P., Rohrbach, P., McLean, J. E., Fidock, D. A., Stein, W. D., and Lanzer, M. (2007) Differences in trans-stimulated chloroquine efflux kinetics are linked to *pfcrt* in *Plasmodium falciparum*. *Mol Microbiol* **64**, 407-420
17. Egan, T. J. (2006) Interactions of quinoline antimalarials with hematin in solution. *J Inorg Biochem* **100**, 916-926
18. Bakouh, N., Bellanca, S., Nyboer, B., Moliner Cubel, S., Karim, Z., Sanchez, C. P., Stein, W. D., Planelles, G., and Lanzer, M. (2017) Iron is a substrate of the *Plasmodium falciparum* chloroquine resistance transporter pfcrt in xenopus oocytes. *J Biol Chem* **292**, 16109-16121
19. Juge, N., Moriyama, S., Miyaji, T., Kawakami, M., Iwai, H., Fukui, T., Nelson, N., Omote, H., and Moriyama, Y. (2015) *Plasmodium falciparum* chloroquine resistance transporter is a H+-coupled polyspecific nutrient and drug exporter. *Proc Natl Acad Sci U S A* **112**, 3356-3361
20. Patzewitz, E. M., Salcedo-Sora, J. E., Wong, E. H., Sethia, S., Stocks, P. A., Maughan, S. C., Murray, J. A., Krishna, S., Bray, P. G., Ward, S. A., and Muller, S. (2013) Glutathione transport: A new role for PfCRT in chloroquine resistance. *Antioxid Redox Signal* **19**, 683-695
21. Summers, R. L., Dave, A., Dolstra, T. J., Bellanca, S., Marchetti, R. V., Nash, M. N., Richards, S. N., Goh, V., Schenk, R. L., Stein, W. D., Kirk, K., Sanchez, C. P., Lanzer, M., and Martin, R. E. (2014) Diverse mutational pathways converge on saturable chloroquine transport *via* the malaria parasite's chloroquine resistance transporter. *Proc Natl Acad Sci U S A* **111**, E1759-E1767
22. Bellanca, S., Summers, R. L., Meyrath, M., Dave, A., Nash, M. N., Dittmer, M., Sanchez, C. P., Stein, W. D., Martin, R. E., and Lanzer, M. (2014) Multiple drugs compete for transport via the *Plasmodium falciparum* chloroquine resistance transporter at distinct but interdependent sites. *J Biol Chem* **289**, 36336-36351
23. Gabryszewski, S. J., Modchang, C., Musset, L., Chookajorn, T., and Fidock, D. A. (2016) Combinatorial genetic modeling of *pfcrt*-mediated drug resistance evolution in *Plasmodium falciparum*. *Mol Biol Evol* **33**, 1554-1570
24. Petersen, I., Gabryszewski, S. J., Johnston, G. L., Dhingra, S. K., Ecker, A., Lewis, R. E., de Almeida, M. J., Straimer, J., Henrich, P. P., Palatulan, E., Johnson, D. J., Coburn-Flynn, O., Sanchez, C., Lehane, A. M., Lanzer, M., and Fidock, D. A. (2015) Balancing drug resistance and growth rates via compensatory mutations in the *Plasmodium falciparum* chloroquine resistance transporter. *Mol Microbiol* **97**, 381-395
25. Summers, R. L., Nash, M. N., and Martin, R. E. (2012) Know your enemy: Understanding the role of *pfcrt* in drug resistance could lead to new antimalarial tactics. *Cell Mol Life Sci* **69**, 1967-1995
26. Lasonder, E., Green, J. L., Camarda, G., Talabani, H., Holder, A. A., Langsley, G., and Alano, P. (2012) The *Plasmodium falciparum* schizont phosphoproteome reveals extensive phosphatidylinositol and camp-protein kinase a signaling. *J Proteome Res* **11**, 5323-5337
27. Solyakov, L., Halbert, J., Alam, M. M., Semblat, J. P., Dorin-Semblat, D., Reininger, L., Bottrill, A. R., Mistry, S., Abdi, A., Fennell, C., Holland, Z., Demarta, C., Bouza, Y., Sicard, A., Nivez, M. P., Eschenlauer, S., Lama, T., Thomas, D. C., Sharma, P., Agarwal, S., Kern, S., Pradel, G., Graciotti, M., Tobin, A. B., and Doerig, C. (2011) Global kinomic and phospho-proteomic analyses of the human malaria parasite *Plasmodium falciparum*. *Nat Commun* **2**, 565
28. Jones, M. L., Collins, M. O., Goulding, D., Choudhary, J. S., and Rayner, J. C. (2012) Analysis of protein palmitoylation reveals a pervasive role in *plasmodium* development and pathogenesis. *Cell Host Microbe* **12**, 246-258
29. Mehrens, T., Lelleck, S., Cetinkaya, I., Knollmann, M., Hohage, H., Gorboulev, V., Boknik, P., Koepsell, H., and Schlatter, E. (2000) The affinity of the organic cation transporter roct1 is increased by protein kinase c-dependent phosphorylation. *J Am Soc Nephrol* **11**, 1216-1224
30. Moritz, A. E., Rastedt, D. E., Stanislowski, D. J., Shetty, M., Smith, M. A., Vaughan, R. A., and Foster, J. D. (2015) Reciprocal phosphorylation and palmitoylation control dopamine transporter kinetics. *J Biol Chem* **290**, 29095-29105
31. Sardet, C., Fafournoux, P., and Pouyssegur, J. (1991) Alpha-thrombin, epidermal growth factor, and okadaic acid activate the Na+/H+ exchanger, NHE-1, by phosphorylating a set of common sites. *J Biol Chem* **266**, 19166-19171

32. Aryal, B., Laurent, C., and Geisler, M. (2015) Learning from each other: Abc transporter regulation by protein phosphorylation in plant and mammalian systems. *Biochem Soc Trans* **43**, 966-974
33. Davies, S. P., Reddy, H., Caivano, M., and Cohen, P. (2000) Specificity and mechanism of action of some commonly used protein kinase inhibitors. *Biochem J* **351**, 95-105
34. Bain, J., McLauchlan, H., Elliott, M., and Cohen, P. (2003) The specificities of protein kinase inhibitors: An update. *Biochem J* **371**, 199-204
35. Dounay, A. B., and Forsyth, C. J. (2002) Okadaic acid: The archetypal serine/threonine protein phosphatase inhibitor. *Curr Med Chem* **9**, 1939-1980
36. Sanchez, C. P., McLean, J. E., Stein, W., and Lanzer, M. (2004) Evidence for a substrate specific and inhibitable drug efflux system in chloroquine resistant *Plasmodium falciparum* strains. *Biochemistry* **43**, 16365-16373
37. Heinberg, A., and Kirkman, L. (2015) The molecular basis of antifolate resistance in *Plasmodium falciparum*: Looking beyond point mutations. *Ann N Y Acad Sci* **1342**, 10-18
38. Ghorbal, M., Gorman, M., Macpherson, C. R., Martins, R. M., Scherf, A., and Lopez-Rubio, J. J. (2014) Genome editing in the human malaria parasite *Plasmodium falciparum* using the CRISPR-Cas9 system. *Nat Biotechnol* **32**, 819-821
39. Summers, R. L., Dave, A., Dolstra, T. J., Bellanca, S., Marchetti, R. V., Nash, M. N., Richards, S. N., Goh, V., Schenk, R. L., Stein, W. D., Kirk, K., Sanchez, C. P., Lanzer, M., and Martin, R. E. (2014) Diverse mutational pathways converge on saturable chloroquine transport via the malaria parasite's chloroquine resistance transporter. *Proc Natl Acad Sci U S A* **111**, E1759-1767
40. Sidhu, A. B., Verdier-Pinard, D., and Fidock, D. A. (2002) Chloroquine resistance in *Plasmodium falciparum* malaria parasites conferred by pfcrt mutations. *Science* **298**, 210-213
41. Antony, H. A., Topno, N. S., Gummadi, S. N., Siva Sankar, D., Krishna, R., and Parija, S. C. (2019) In silico modeling of *Plasmodium falciparum* chloroquine resistance transporter protein and biochemical studies suggest its key contribution to chloroquine resistance. *Acta Trop* **189**, 84-93
42. Ciarimboli, G., Koepsell, H., Iordanova, M., Gorboulev, V., Durner, B., Lang, D., Edemir, B., Schroter, R., Van Le, T., and Schlatter, E. (2005) Individual PKC-phosphorylation sites in organic cation transporter 1 determine substrate selectivity and transport regulation. *J Am Soc Nephrol* **16**, 1562-1570
43. Saitoh, M., Ishikawa, T., Matsushima, S., Naka, M., and Hidaka, H. (1987) Selective inhibition of catalytic activity of smooth muscle myosin light chain kinase. *J Biol Chem* **262**, 7796-7801
44. Holland, Z., Prudent, R., Reiser, J. B., Cochet, C., and Doerig, C. (2009) Functional analysis of protein kinase CK2 of the human malaria parasite *Plasmodium falciparum*. *Eukaryot Cell* **8**, 388-397
45. Umeda, D., Yamada, K., and Tachibana, H. (2008) H89 (n-[2-(p-bromocinnamylamino)ethyl]-5-isoquinolinesulfonamide) induces reduction of myosin regulatory light chain phosphorylation and inhibits cell proliferation. *Eur J Pharmacol* **590**, 61-66
46. Yamaki, T., Tanaka, T., and Hidaka, H. (1979) [platelet cyclic nucleotides and calcium]. *Rinsho Byori* **Suppl 40**, 67-73
47. Zimmer, M., Gobel, C., and Hofmann, F. (1984) Calmodulin activates bovine-cardiac myosin light-chain kinase by increasing the affinity for myosin light-chain 2. *Eur J Biochem* **139**, 295-301
48. Lucet, I. S., Tobin, A., Drewry, D., Wilks, A. F., and Doerig, C. (2012) Plasmodium kinases as targets for new-generation antimalarials. *Future Med Chem* **4**, 2295-2310
49. Trager, W., and Jensen, J. B. (1976) Human malaria parasites in continuous culture. *Science* **193**, 673-675
50. Lambros, C., and Vanderberg, J. P. (1979) Synchronization of *Plasmodium falciparum* erythrocytic stages in culture. *J Parasitol* **65**, 418-420
51. Ho, S. N., Hunt, H. D., Horton, R. M., Pullen, J. K., and Pease, L. R. (1989) Site-directed mutagenesis by overlap extension using the polymerase chain reaction. *Gene* **77**, 51-59
52. Wu, Y., Sifri, C. D., Lei, H. H., Su, X. Z., and Wellems, T. E. (1995) Transfection of *Plasmodium falciparum* within human red blood cells. *Proc Natl Acad Sci U S A* **92**, 973-977

53. Sanchez, C. P., Stein, W., and Lanzer, M. (2003) Trans stimulation provides evidence for a drug efflux carrier as the mechanism of chloroquine resistance in *Plasmodium falciparum*. *Biochemistry* **42**, 9383-9394
54. Smilkstein, M., Sriwilaijaroen, N., Kelly, J. X., Wilairat, P., and Riscoe, M. (2004) Simple and inexpensive fluorescence-based technique for high-throughput antimalarial drug screening. *Antimicrob Agents Chemother* **48**, 1803-1806
55. Lin-Moshier, Y., and Marchant, J. S. (2013) A rapid Western blotting protocol for the *Xenopus* oocyte. *Cold Spring Harb Protoc* **2013**, 10.1101/pdb.prot072793

Table 1. Kinetic parameters for chloroquine transport of $PfCRT^{Dd2}$ and Ser-33 mutants. Best-fit values of kinetic parameters were obtained from the kinetics of chloroquine uptake depicted in Fig. 7C, using the Michaelis Menten equation. Statistical differences between the kinetic curves were analyzed in relation to Dd2 using F-statistics and between kinetic parameters using the Holm-Sidak one way ANOVA test.

	Apparent K_m (μM)	Apparent V_{max} (pmol $oocyte^{-1}$ h^{-1})	p value (F value, degrees of freedom)
$PfCRT^{Dd2}$	250 ± 40	33 ± 3	-
$PfCRT^{S33A}$	230 ± 45	22 ± 2*	2.3×10^{-7} (F=71, DF=14)
$PfCRT^{S33E}$	200 ± 15	26 ± 1	6.2×10^{-5} (F=24, DF=14)
$PfCRT^{S33D}$	215 ± 20	33 ± 2	4.0×10^{-2} (F=4, DF=14)

* versus $PfCRT^{Dd2}$ p = 0.012, versus $PfCRT^{S33D}$ p = 0.006 , according to Holm-Sidak one way ANOVA.

Table 2. Chloroquine efflux rates from *P. falciparum* Dd2 and PfCRT Ser-33 mutant parasites. Best-fit values of kinetic parameters were obtained from the kinetics of chloroquine (CQ) efflux depicted in Fig. 7D, by fitting a single, three parameter exponential decay equation to the data points. Statistical differences between the kinetic curves were analyzed using F-statistics in relation to Dd2 and between kinetic parameters using the Holm-Sidak one way ANOVA test.

	Initial CQ efflux rate (min^{-1})	p value (F value, degrees of freedom)
Dd2	0.71 ± 0.03	-
B6 S33A	0.43 ± 0.04*	1.5×10^{-4} (F=46, DF=9)
C8 S33E	0.61 ± 0.05	0.37 (F=1, DF=9)
G8 S33D	0.68 ± 0.04	0.45 (F=1, DF=9)

* versus Dd2 $p < 0.001$, versus C8 S33E $p = 0.018$, versus G8 S33D $p = 0.001$ according to Holm-Sidak one way ANOVA.

Figure 1. MS/MS spectra of PfCRT^{Dd2} tryptic phosphopeptides. *A*, CID mass spectrum of the triply charged tryptic phosphopeptide Y20-R34 (m/z 610.64). After database searching, the peptide was identified as containing a single phosphorylation at residue Ser-33. *B*, CID mass spectrum of the triply charged tryptic phosphopeptide N405-R426 containing the residue Ser-411. The presence of fragments b10 and b11 confirmed that Ser-411 is phosphorylated. The phosphorylated residues are indicated by PH.

Figure 2. Effect of protein kinase and phosphatase inhibitors on chloroquine responsiveness in *P. falciparum*. *A,* The level of [^{3}H]-chloroquine accumulation from an extracellular chloroquine concentration of 43 nM, given as the ratio of the intracellular versus extracellular chloroquine concentration (CQ_{in}/CQ_{out}), was determined after 5 min in the presence of different protein kinase and phosphatase inhibitors. Inhibitors were used at the concentrations, in micromolar, indicated in parenthesis. The chloroquine accumulation ratios were expressed in relation to that of untreated Dd2. A box plot analysis is overlaid over the individual data points (independent biological replicates), with the median, the mean (red line) and the 25% and 75% quartile ranges being shown. Statistical significance was assessed using the Student's t-test in reference to Dd2. *B,* The level of chloroquine accumulation after 5 min of incubation as a function of increasing concentrations of ML-7. The means ± SEM of n=3-4 independent biological replicates are shown. *C,* Effect of increasing concentrations of ML-7 on parasite growth, as determined in a standard cell proliferation assay with a drug exposure time of 72 h. The means ± SEM of n=4 independent biological replicates are shown. Dd2, chloroquine resistant *P. falciparum* strain (white symbols). HB3, chloroquine sensitive strain (grey symbols).

Figure 3. Effect of ML-7 on drug responses in *P. falciparum*. *A,* Chloroquine, *B,* quinine, and *C,* pyrimethamine IC_{50} values for *P. falciparum* strains Dd2 (white symbols) and HB3 (grey symbols) in the presence and absence of 2.5 μM ML-7. Each symbol represents an independent biological replicate. A box plot analysis is overlaid over the individual data points, with the median, the mean (red line) and the 25% and 75% quartile ranges being shown. Statistical significance was assessed using the Student's t-test.

Figure 4. Site directed mutagenesis of *pfcrt* via CRISPR/Cas9-mediated genome editing technology. *A,* Transfection strategy. A double strand break was introduced into the genomic *pfcrt* gene via a site-specific Cas9 endonuclease (vector expressing Cas9 is not shown nor is the Cas9 guide RNA). The double strand break was subsequently repaired by double homologous recombination using a fragment (from position -137 to 778 of *pfcrt*) containing the appropriate mutational changes leading to the substitution of alanine, aspartic acid, or glutamic for serine 33. *B,* Chromatograms showing the sequencing reads across the mutagenized region of the *pfcrt* gene. The sequenced DNA was obtained by PCR amplification of genomic DNA from the indicated mutants.

Figure 5. Localization, expression and stability of mutated PfCRT variants in *P. falciparum*. *A,* Immuno-fluorescence images of Dd2 (upper panels) and the PfCRT mutants indicated stained with a rabbit anti-PfCRT antiserum (1:1000 dilution). As a secondary antibody a donkey anti-rabbit Alexa Fluor 488 antibody was used (1:1000 dilution). Left image, PfCRT fluorescence signal; middle image, differential interference contrast (DIC); right image, overlay of both images. Scale bar: 2 μm. *B,* Western blot analyses of total protein derived from trophozoites, using a rabbit anti-PfCRT antiserum and, as a loading control, a mouse monoclonal anti-tubulin antibody. The luminescence signals from independent Western analyses were quantified and the PfCRT specific signals were normalized to that of tubulin. Each symbol represents an independent biological replicate. A box plot analysis is overlaid over the individual data points, with the median, the mean (red line) and the 25% and 75% quartile ranges being shown. No differences in PfCRT steady state expression levels were observed between the Dd2 and the PfCRT S33 mutants, according to Holm-Sidak one way ANOVA test. The different PfCRT mutants are indicated. A protein size standard is indicated in kDa.

Figure 6. Drug responses of the PfCRT S33 mutants. The IC_{50} values of the PfCRT S33 mutants, the parental strain Dd2 and the chloroquine sensitive strain HB3 are shown for chloroquine (CQ),

chloroquine in the presence of 0.89 μM verapamil (CQ + VP), quinine (QN), and pyrimethamine (PYR). Each symbol represents an independent biological replicate. A box plot analysis is overlaid over the individual data points with the median and the 25% and 75% quartile ranges being shown. Statistical significance was determined using the Holm-Sidak one way ANOVA test. The p-values obtained are indicated.

Figure 7. Effect of PfCRT S33 mutations on chloroquine uptake kinetics and efflux. *A,* Immuno-fluorescence images of fixed $PfCRT^{Dd2}$- and $PfCRT^{S33X}$-expressing oocytes and water-injected control oocytes. *Left,* fluorescence image of PfCRT using a specific guinea-pig antiserum and the Alexa Fluor 488 anti-guinea pig secondary antibody. *Middle,* fluorescence image of $InsP_3R$, using a specific rabbit antiserum and an Alexa Fluor 546 anti-rabbit secondary antibody. *Right,* differential interference contrast image. Scale bar: 125 μm. *B,* Western blot analyses of total lysates from oocytes injected with water, $PfCRT^{Dd2}$ or $PfCRT^{S33X}$ RNA, using the polyclonal guinea pig antiserum specific to PfCRT and, as a loading control, mouse monoclonal anti-tubulin antibody. The luminescence signals from four independent Western blot analyses were quantified, yielding the PfCRT expression levels relative to the internal standard α–tubulin. A box plot analysis is overlaid over the individual data points (independent biological replicates), with the median, the mean (red line) and the 25% and 75% quartile ranges being shown. A size standard is indicated in kilodaltons. *C,* Kinetics of chloroquine uptake by oocytes expressing either $PfCRT^{Dd2}$ (yellow circle), $PfCRT^{S33A}$ (orange triangle), $PfCRT^{S33E}$ (green triangle) or $PfCRT^{S33D}$ (blue square). Water-injected oocytes were investigated in parallel and the chloroquine uptake values were subtracted from those of PfCRT-expressing oocytes. Chloroquine uptake is shown as the mean ± SEM of n=4-6 independent biological replicates, with N=10 oocytes per treatment and biological replicate. The Michaelis Menten equation was fitted to the data points and the kinetic parameters obtained were compiled in Table 1. *D,* Time courses of chloroquine efflux from *P. falciparum*-infected erythrocytes pre-loaded with [^{3}H]-chloroquine. The amount of intracellular chloroquine remaining (CQ_{in}) was normalized to the value obtained at time point zero. The mean ± SEM of n>4 independent biological replicates are shown. The initial chloroquine efflux rate was obtained by fitting a single, three parameter exponential decay equation to the data points (Table 2). The *P. falciparum* strain Dd2 and the PfCRT S33 mutants investigated are indicated (symbol and color code, see above).

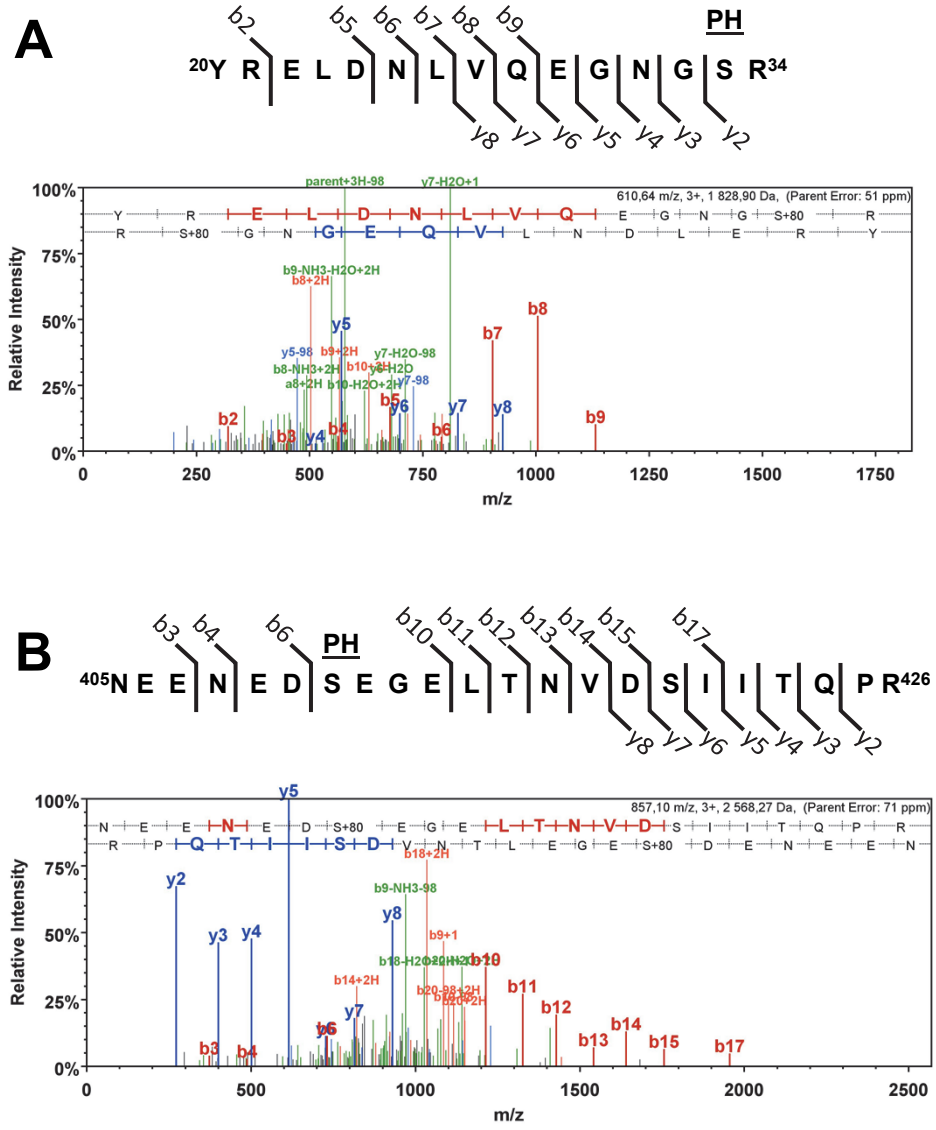

Figure 1

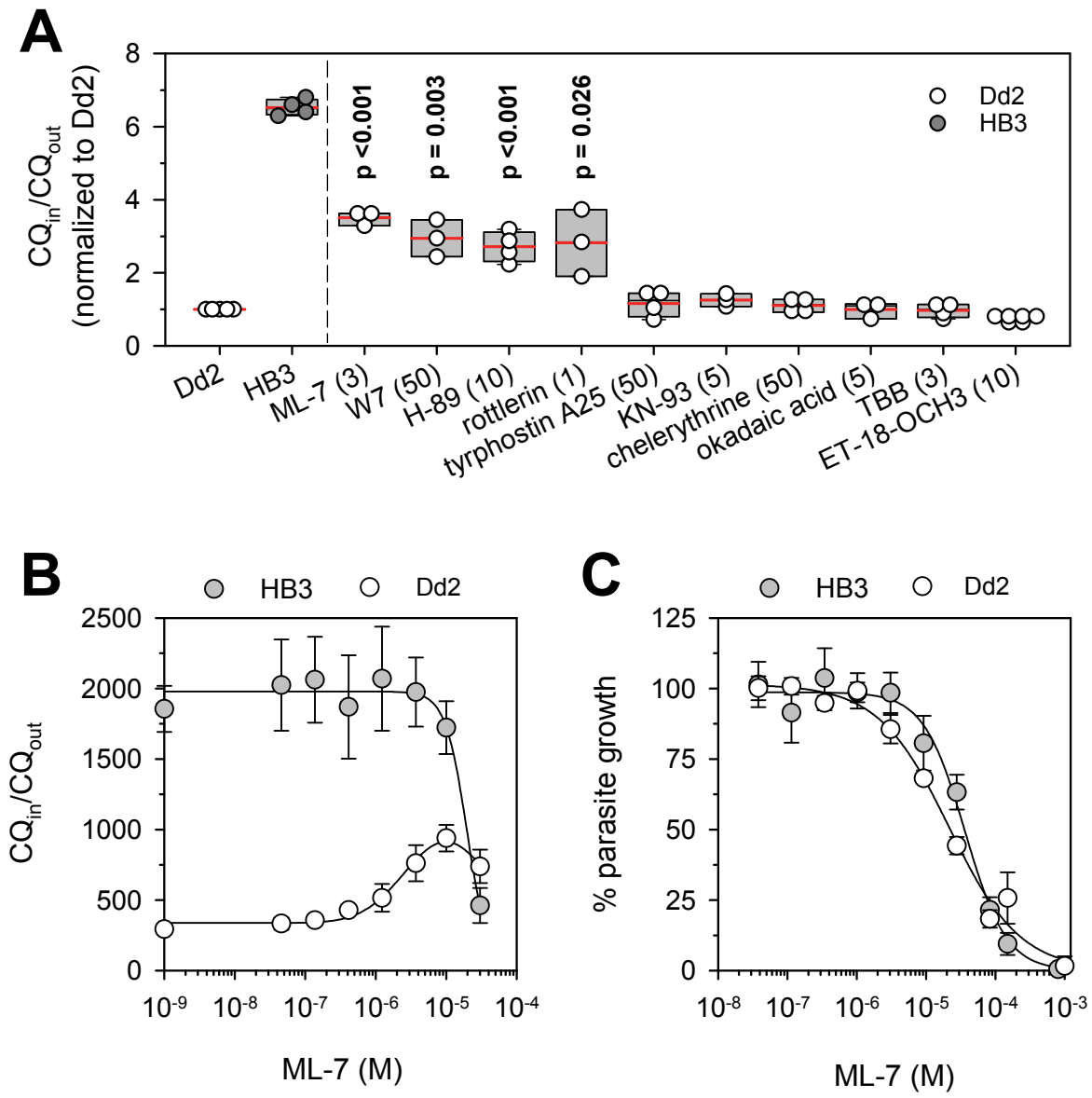

Figure 2

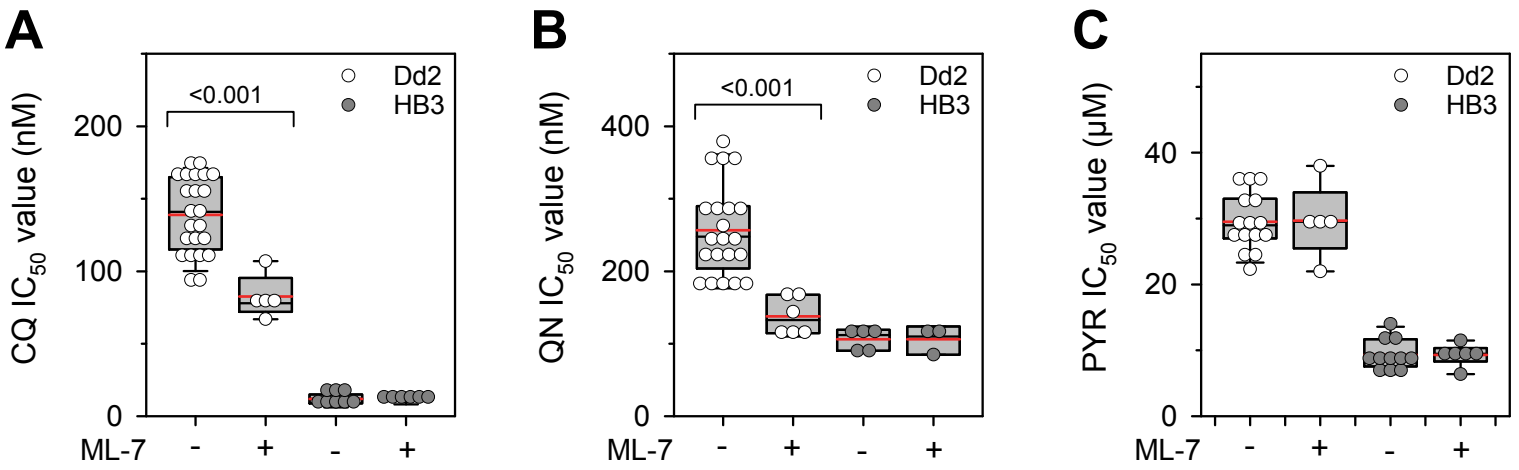

Figure 3

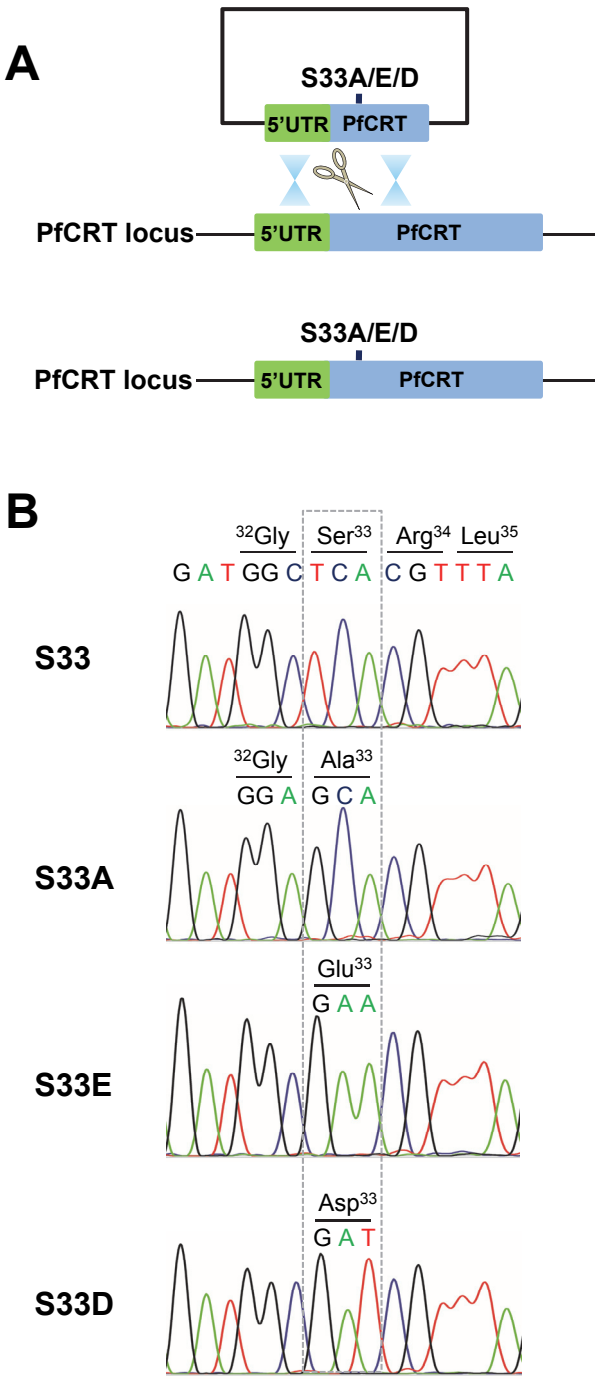

Figure 4

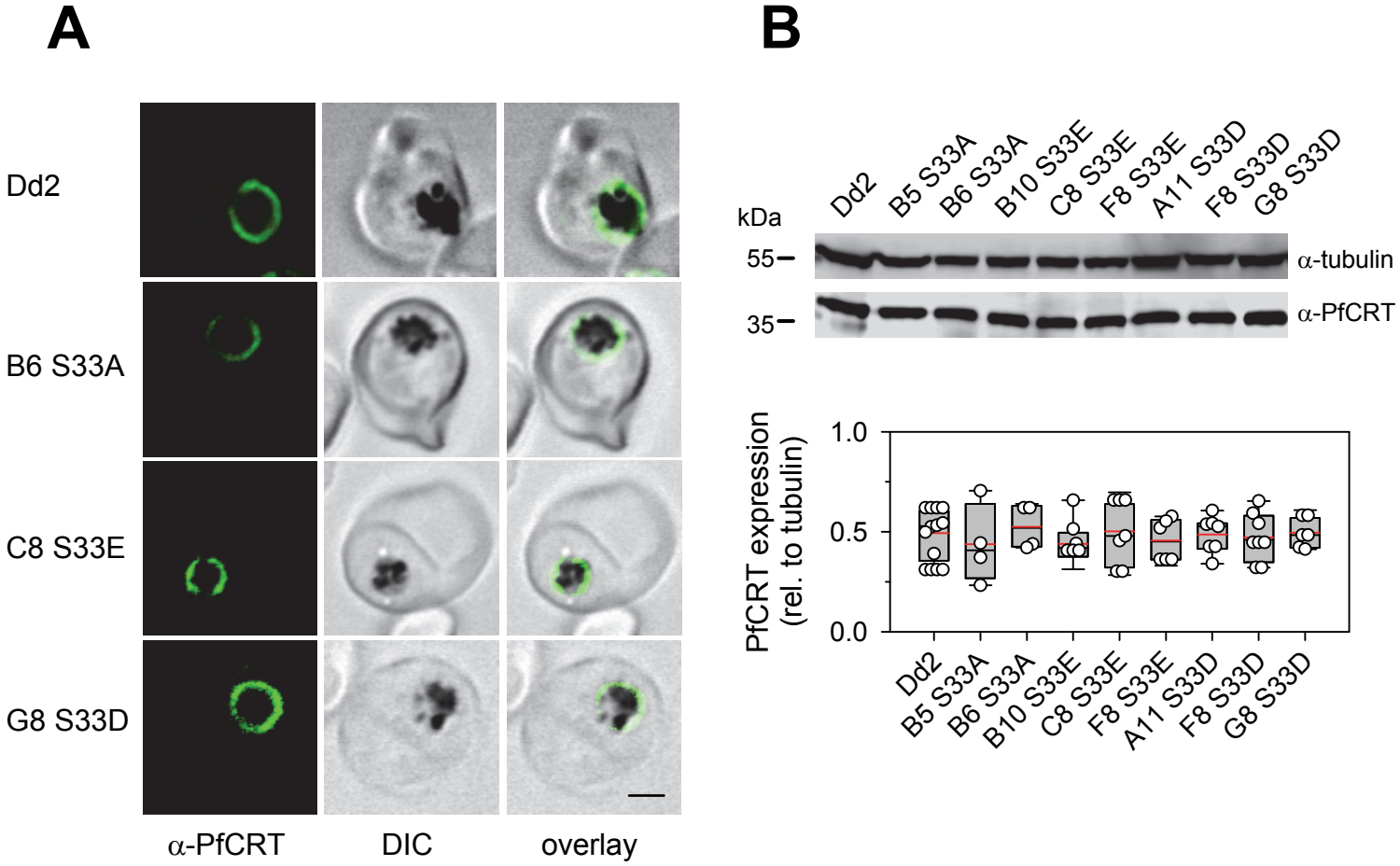

Figure 5

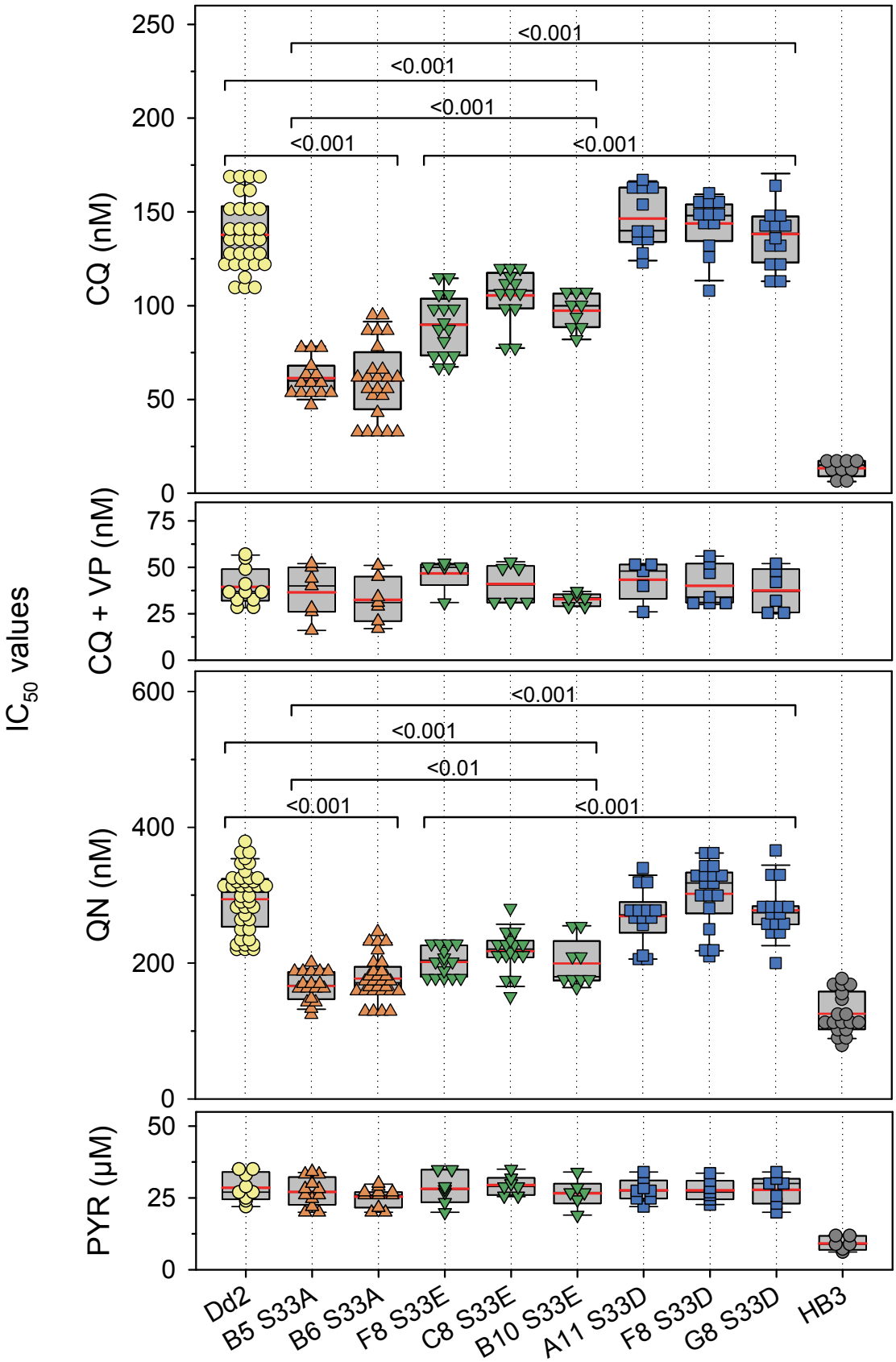

Figure 6

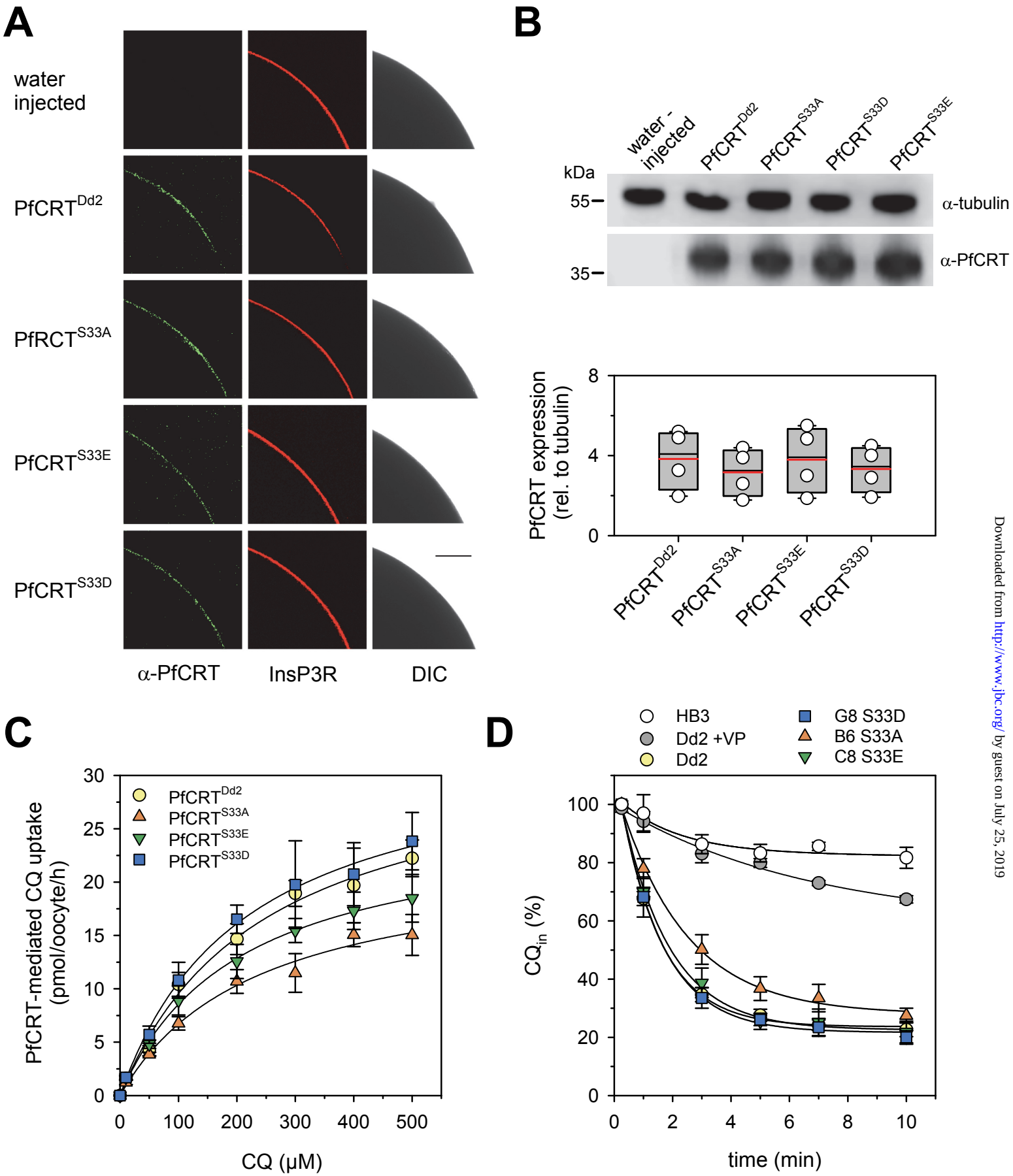

Figure 7

Phosphomimetic substitution at Ser-33 of the chloroquine resistance transporter PfCRT reconstitutes drug responses in *Plasmodium falciparum*

Cecilia P. Sanchez, Sonia Moliner Cubel, Britta Nyboer, Monika Jankowska-Döllken, Christine Schaeffer-Reiss, Daniel Ayoub, Gabrielle Planelles and Michael Lanzer

J. Biol. Chem. published online July 8, 2019
